

Role of dielectric properties in terahertz field transmission

Cite as: J. Appl. Phys. **117**, 223109 (2015); <https://doi.org/10.1063/1.4922629>

Submitted: 03 March 2015 • Accepted: 05 June 2015 • Published Online: 12 June 2015

Minah Seo, Joong Wook Lee and Hwi Kim



View Online



Export Citation



CrossMark

ARTICLES YOU MAY BE INTERESTED IN

[Terahertz field confinement and enhancement in various sub-wavelength structures](#)

Journal of Applied Physics **126**, 120901 (2019); <https://doi.org/10.1063/1.5110046>

[Terahertz conductivity of thin metal films](#)

Applied Physics Letters **93**, 051105 (2008); <https://doi.org/10.1063/1.2968308>

[Tutorial: An introduction to terahertz time domain spectroscopy \(THz-TDS\)](#)

Journal of Applied Physics **124**, 231101 (2018); <https://doi.org/10.1063/1.5047659>



Applied Physics
Reviews

Read. Cite. Publish. Repeat.

19.162

2020 IMPACT FACTOR*



Role of dielectric properties in terahertz field transmission

Minah Seo,^{1,a)} Joong Wook Lee,² and Hwi Kim³

¹*Sensor System Research Center, Korea Institute of Science and Technology, Seoul 136-791, South Korea*

²*Department of Physics and Optoelectronics Convergence Research Center, Chonnam National University, Gwangju 500-757, South Korea*

³*ICT Convergence Technology for Health & Safety, Department of Electronics and Information Engineering, Korea University, 2511 Sejong-ro, Sejong 339-700, South Korea*

(Received 3 March 2015; accepted 5 June 2015; published online 12 June 2015; publisher error corrected 30 June 2015)

We compare the field transmission characteristics of a freestanding perforated metal film (as a conductor) and a polymethylmethacrylate–graphite composite film (as an absorber) in the terahertz frequency range. The role of dielectric properties of the materials and the contribution of surface waves toward enhanced transmission with periodic and random hole arrays are discussed. Periodic subwavelength hole arrays in metal films do support enhanced terahertz field transmission whereas random arrays do not. In contrast, neither periodic nor random arrays of subwavelength holes punctured in dielectric absorbers support such transmission. Notably, even a dielectric absorber with large holes, which is sufficiently larger than subwavelength holes, can result in features in transmission due to the shape resonance, but the effect is very small. © 2015 AIP Publishing LLC.

[<http://dx.doi.org/10.1063/1.4922629>]

I. INTRODUCTION

Transmission enhancement using both one-dimensional (1D) and two-dimensional (2D) arrays of subwavelength holes in optically thick metallic films^{1–3} has received considerable attention in related applications, e.g., perfect transmission in perfect conductors with apertures,⁴ and recently pioneered metamaterials.^{5,6} Recent observations of enhanced transmission have been experimentally demonstrated using subwavelength apertures in doped silicon and metallic films even at terahertz (THz) frequencies,^{7,8} and using an active THz device employing electron beams coupled to a transmission grating.⁹ These phenomena of enhanced transmission have been explained thus as: a perforated conductor induces transmission supported by surface plasmon polaritons (SPPs) or plasmon-like surface waves, which are assisted by the conductor geometry.^{10,11} Also, surface waves sustained by a thin dielectric layer play a clear role in enhancement of transmission.¹¹ An intriguing aspect of dielectric properties is that enhanced transmission is influenced by the occurrence of surface waves upon varying the dielectric properties. Varying the dielectric properties of a substrate film with a hole array¹² essentially provides control over the resonance frequency of transmission. Moreover, total transmission, normalized to an open fraction, increases in the presence of hole arrays supported by surface waves upon a conductor film or in the presence of large-sized holes. The current intense research interest in plasmonic materials in the THz region^{13–16} necessitates the understanding of the dielectric response of various materials that support resonant behavior. Recently, introduced metal-dielectric composite films^{17,18} can assist in overcoming the lack of dielectric properties.

Thus, an investigation of the effect of surface waves on transmission resonance is required.

In this report, we show whether dielectric properties and surface waves generated by dielectric constant engineering with periodic and random holes contribute to transmission enhancement in the THz region. By using both a far field THz time-domain spectroscopy (TDS) system and a near field THz imaging system, we report experimentally that hole arrays in dielectric films have only direct transmission above the first Rayleigh minimum. This is in contrast to metallic films that show enhanced transmissions.¹⁹ In order to accurately quantify the role of surface waves sustained by this system in transmission enhancement, polymethylmethacrylate (PMMA) film with graphite powder as an absorber and aluminum foil as a conductor were considered. We show that periodic arrays of subwavelength holes in metal films do support enhanced THz transmission whereas random arrays do not. In contrast, neither periodic nor random arrays of subwavelength holes punctured in dielectric absorbers support enhanced THz transmission. In addition, we show that large-sized holes, ensuring the shape resonance effect dominantly,²⁰ have barely distinguishable features even in the case of an absorber film. This observation supports the fact that the shape of structures, including size effects, strongly contributes to the enhancement of transmission in designed frequency regions.

II. EXPERIMENT AND SAMPLE PREPARATION

While pure graphite is metallic in the experimentally reliable THz region from 0.1 THz to 1.65 THz, PMMA is transparent and dielectric in this region. However, a composite of graphite and PMMA mixed in appropriate amounts can be an excellent terahertz absorber that shows good shielding efficiency and small reflection in this region. Our dielectric absorber film consists of a PMMA host with embedded

^{a)}Author to whom correspondence should be addressed. Electronic mail: mseo@kist.re.kr.

graphite particles, which has a specific dielectric property which is determined by the graphite concentrations. The PMMA-graphite composite has a graphite concentration of 35.7 wt.%, and shows a reflection of less than 10% and absorption of over 80% at high frequencies (>1 THz), which makes this material essentially “black.”¹⁷ We fabricated arrays with periodic arrangement (radius $a = 190 \mu\text{m}$ and $400 \mu\text{m}$ with period $d = 613 \mu\text{m}$) and circular holes with the same areal coverage on the PMMA-graphite composite film (thickness $h = 300 \mu\text{m}$) but without periodicity, punctured by the femtosecond laser machining method. We have also studied the THz transmission properties with periodic and random arrays of circular holes ($a = 223 \mu\text{m}$ and $400 \mu\text{m}$ with $d = 625 \mu\text{m}$) on an aluminum foil ($h = 17 \mu\text{m}$).

In order to get an insight on the role of surface waves, a comparison between a metal and an absorber at THz frequency is essential. The PMMA-graphite composite film as an absorber including circular holes is shown in Fig. 1(a). The weight ratio of graphite is 35.7 wt.%, which is the maximum fraction that sustains a freestanding film state. Dielectric properties calculated from complex refractive indices obtained from a THz transmission experiment are shown in Fig. 1(b), where graphite concentration is 35.7 wt.%. In the PMMA host, heterogeneously distributed graphite powders play an important role in THz absorption owing to charge localization, while electromagnetic waves pass through the metal islands.^{17,21} Absorptive films can accelerate surface wave attenuation, as might be expected from the postulation of Martens *et al.* that Drude free carrier response gives a very short scattering time on the order 10 fs.²² The absorber film provides a control experiment to study the existence and role of surface waves in the field enhancement of transmission.

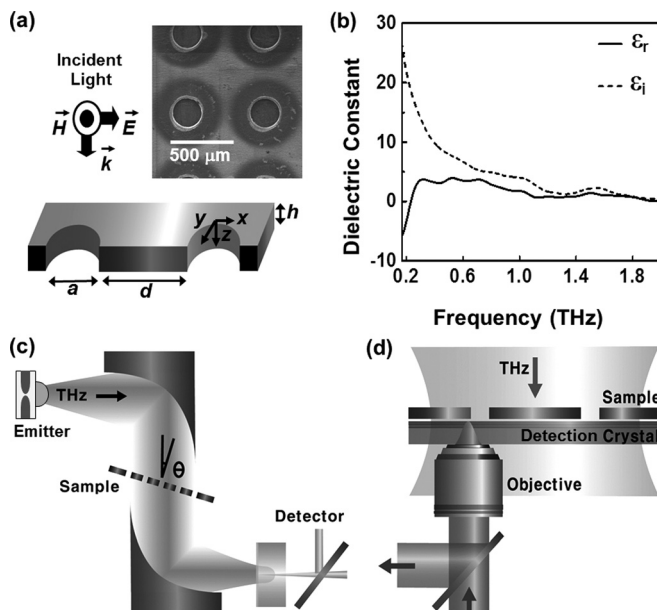


FIG. 1. (a) Schematic view of two-dimensional material and SEM image of perforated PMMA-graphite composite film. (b) Real and imaginary parts of dielectric constant of PMMA-graphite composite were analyzed from THz transmission data. Weight concentration of graphite is 35.7 wt.%, which results in largest absorption and lowest transmission. (c) Angle-dependent transmission spectra were measured by rotating the sample holder. (d) Near-field THz imaging setup is shown.

To measure the dielectric response and transmission of perforated samples in the THz region, THz TDS was used. In our experiments, we used GaAs crystal, which has a high resistivity ($\rho > 10^7 \Omega\text{m}$), and irradiated the emitter with 150 fs pulses at the center wavelength of $\lambda = 800 \text{nm}$. Meanwhile, a pulsed high voltage (280 V, 50 kHz) was applied to the electrodes to generate broadband THz waves at 0.05–1.8 THz (Fig. 1(c)). Samples were mounted at a rotation holder to get angle dependent transmission spectra. In order to detect THz waves, a balanced detection system was used for electro-optic sampling using a ZnTe crystal. On the other hand, to obtain near-field images at the surfaces of these samples, the apertureless type of THz near-field technique, which directly images the surface of a sample within the subwavelength regime, was also used (Fig. 1(d)).²³ For near-field measurement, the sample should be directly attached to the detection crystal. While the THz wave approaches from one side, and was normally incident to the surface of the interface between the sample and detection crystal, optical probe beam polarization was changed by the THz field at the sample-crystal interface and was reflected back toward the differential detection setup. We measured the vertical component (z -component) of the electric field for near-field imaging because this component is responsible for charge density at the sample surface. This can provide a way for direct examination of surface waves. To measure the z -component of the electric field, a (100)-oriented GaP crystal was used.²⁴

III. RESULTS AND DISCUSSION

In order to compare the scattered field profiles due to the existence of surface waves, we measured the transmissions of both absorptive and metallic materials with subwavelength hole arrays, in the spectral range of 0.05–1.65 THz (Fig. 2). The hole sizes for the metal and absorptive films were $223 \mu\text{m}$ and $190 \mu\text{m}$, respectively. The spectra were obtained by a fast Fourier transform method, and were normalized by dividing them with the reference signal though an empty square aperture of $20 \times 20 \text{mm}^2$. Moreover, we investigated the contributions of periodicity on the materials by contrasting them with randomly perforated features in the case of absorptive and metallic films. As proven in several recent studies,^{8,24} we first confirmed the existence of a transmission minimum at $f_{\text{Res}} = c/d = 0.5 \text{THz}$ in the case of $d = 600 \mu\text{m}$, which corresponds to the first Rayleigh minimum for normal incidence.²⁰ The transmittance in the spectral region above the first Rayleigh minimum was roughly equal to the sample coverage in both metal films (Fig. 2(a)) and absorber films (Fig. 2(b)). In particular, we noted that the transmitted field amplitude was more than 25% even though the hole coverage was very small ($<10\%$) at the peak frequency of 0.46 THz (Fig. 2(a)). This suggests extraordinary enhancement of transmission. This phenomenon was appeared only at the metal samples because of the existence of surface waves. The subsequent prominent transmission peaks were in good agreement with the SPP wavelength model¹⁹ and the Rigorous Coupled Waves Analysis (RCWA) simulation result with diffraction orders at reliable frequencies.

However, the metal sample with random holes and the absorptive material with both periodic and random holes

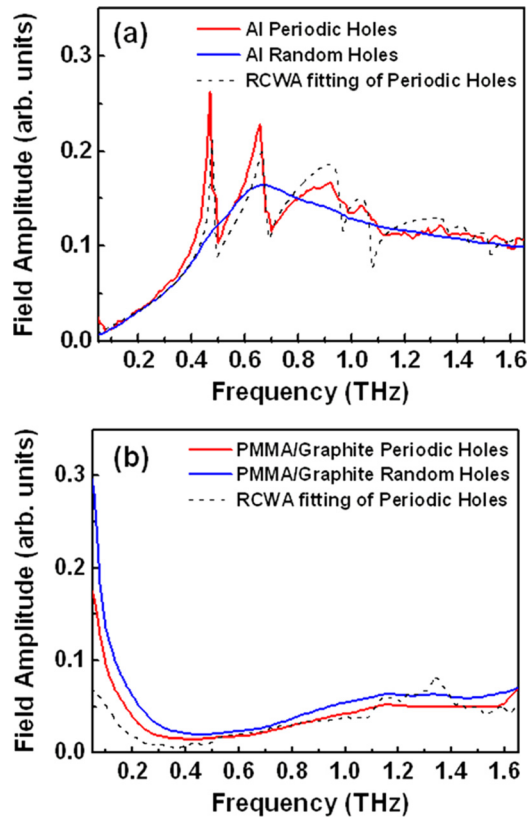


FIG. 2. (a) Normalized transmitted field amplitude spectra of aluminum film with $a = 223 \mu\text{m}$ holes with periodic arrangement (red) and random arrangement (blue). (b) Normalized transmitted field amplitude spectra of PMMA-graphite film with $a = 190 \mu\text{m}$ with periodic arrangement (red) and random arrangement (blue). Short dashed lines represent fitting results obtained from RCWA simulation.

showed a smooth featureless spectrum, as shown in Figs. 2(a) and 2(b), respectively. These results were obtained when the surface of the absorptive material has optimal thickness to minimize scattering, due to the destructive interferences between the incident wave and scattered waves at

the surface of absorptive film. It has been already established that scattering reduction occurs in the case of a randomly rough surface, which is practically equivalent to an increase in absorption.^{25,26} In our PMMA-graphite absorber film, owing to randomly distributed metallic islands within the film, passed THz waves can effectively feel rough surface near the holes that act destructively and result in interference. At this relatively small hole size, surface properties dominantly contribute to the enhancement of transmission. Owing to the fact that the cutoff frequency is sufficiently high in the case of a small hole size, various evanescent surface modes can couple with each other at the metal surface. All experimental results shown in Figs. 2(a) and 2(b) are in excellent agreement with theoretical calculations, as shown by dotted lines obtained from a RCWA-method-based simulation.²⁷ This analytic calculation confirms the experimental findings that transmission enhancement occurs according to surface properties differently.

Previous work on the band structure measurements in periodic and random rectangle hole arrays suggested that strong enhanced THz transmission through the metal film with periodic hole array is clearly incident-angle independent.²⁸ To confirm the clear role of periodicity in our cases, we investigated the angle dependent transmission spectrums between 0° – 35° for above-considered systems. Fig. 3 shows the contour plots of the angle-dependent transmission spectra for Al and PMMA-graphite films with periodic and random holes of a small size. Since the surface wave dispersion relation depends on the dielectric constant and periodicity simultaneously, each material and existence of a period can influence on the results differently. Only periodic structures on the metallic surface can make couplings completely in the evanescent region, leading to clear sharp peaks at 0.45 THz at normal incidence and 0.6 THz at 10° (Fig. 3(a)). The result for the periodic holes represents sharp transmission lines locate at just below the Rayleigh minima frequency lines at $f(\theta) = c/(d(1 \pm \sin\theta))$, where θ is the incident angle. In stark contrast to (a), Al film with random arrays did not

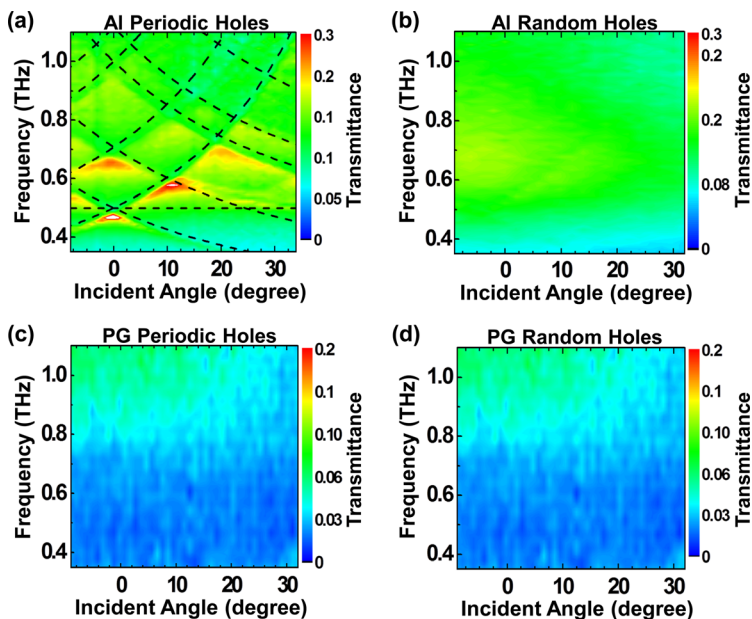


FIG. 3. (a) Angle-dependent transmittance spectra of Al film with holes of $223 \mu\text{m}$ show surface plasmon polariton modes due to various diffraction orders. Dashed lines were calculated Rayleigh lines for various diffraction orders. Angle-dependent transmittance spectra of Al film with random holes of $223 \mu\text{m}$ (b), PMMA-graphite composite with periodic holes of $190 \mu\text{m}$ (c), and random holes (d) are smooth and featureless.

support the strong couplings on the materials in the evanescent region in any angle (Fig. 3(b)). All cases of the PMMA-graphite film with and without periodicity do not support any transmission enhancements in the measurable region due to the lack of the surface waves as expected (Figs. 3(c) and 3(d)).

Differences can also be observed in the cross-sectional views of the measured near-field images (Fig. 4). Using the terahertz near-field apertureless technique,²³ the near-field images were obtained at the surface of the Al hole array at various frequencies: 0.46 THz (Fig. 4(a)) corresponding to the sharp peak position in the far-field spectrum (Fig. 2(a)), 0.5 THz (Fig. 4(b)) corresponding to the Rayleigh minimum (Fig. 2(a)), and 1.5 THz (Fig. 4(c)). The near-field images of the PMMA-graphite films were also measured at 0.46 THz (Fig. 4(d)), 0.5 THz (Fig. 4(e)), and 1.5 THz (Fig. 4(f)). The inset figures below the corresponding near field images represent the calculated image results around the holes by the RCWA method. Both experiments and simulations were carried out only on the periodic holes of Al and PMMA-graphite samples.

These near-field images strongly support the existence of surface waves on the Al film, resulting in the development of a surface plasmon like field distributions in a perfect conductor.¹⁰ We can see clear surface waves developed only around the Al holes (Figs. 4(a) and 4(b)) and not around the absorber holes (Figs. 4(d) and 4(e)) at lower frequencies. The surface

waves are connected hole-to-hole with each other, and the stream of surface waves result from the periodic holes of metals. Exceptionally, the high-frequency images of both the Al hole array (Fig. 4(c)) and PMMA-graphite hole array (Fig. 4(f)) show direct field propagation around the holes. The field distributions are similar owing to dipole radiation around each hole. However, a too short wavelength in this frequency region cannot reach the neighboring hole region, indicating that cannot couple with each other.

With an increase in the hole size, the central frequency of the transmitted peak amplitude shifts toward lower frequency while maintaining the minimum position (f_{Res}), which is related to the period, d (Fig. 5(a)). It should be noted that the first diffraction contributes dominantly to total transmission because this large hole has a lower cutoff frequency than that of the small holes, in contrast to the transmission case of small holes. Furthermore, surprisingly, the PMMA-graphite composite can also produce little features near the minimum frequency f_{Res} (Fig. 5(b)). Clearly, this behavior in the case of large holes should be explained differently from that in the case of small holes, as shown in Fig. 2. This opposite behavior follows shape resonance strongly, which has been introduced in the previous reports,^{20,28,29} indicating fundamental resonance from the hole geometry. It is notable that shape resonance occurs even on the PMMA-graphite film with a large hole array even though the effect is very small.

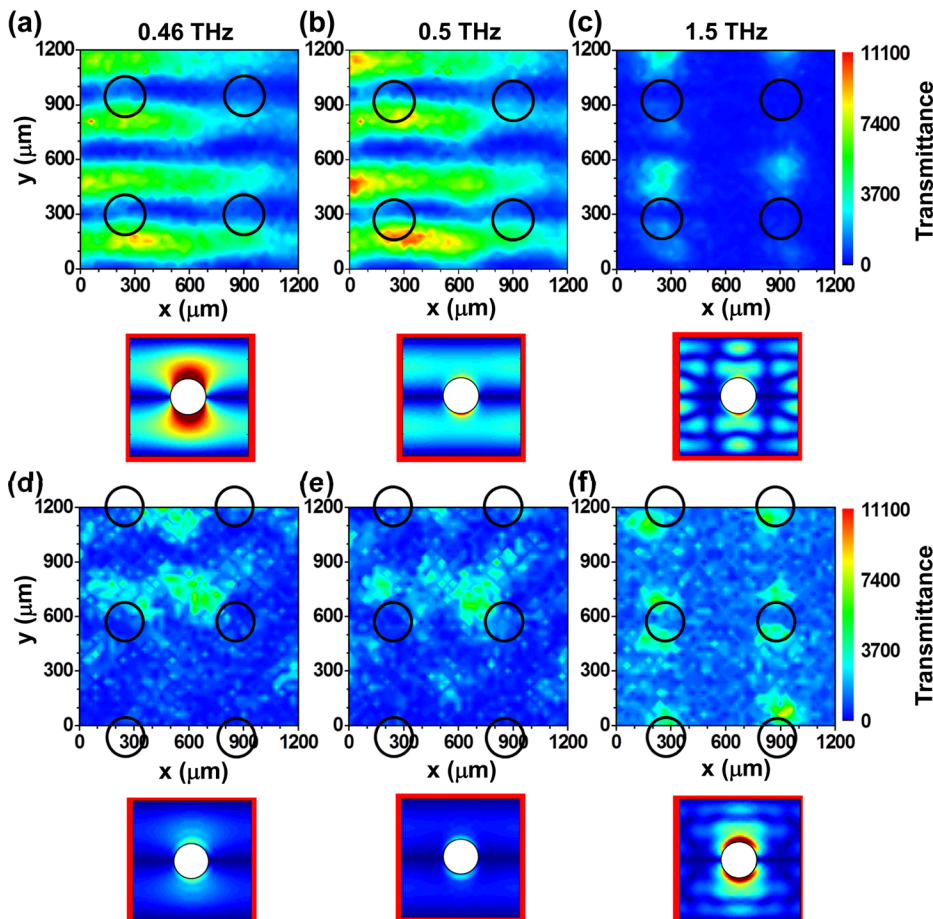


FIG. 4. Near-field profiles at the surface of Al film (a)–(c) and PMMA-graphite film (d)–(f), measured at 0.46 THz ((a) and (d)), 0.5 THz ((b) and (e)), and 1.5 THz ((c) and (f)). Simulations obtained from RCWA method are represented below; these correspond to experimental data at each case.

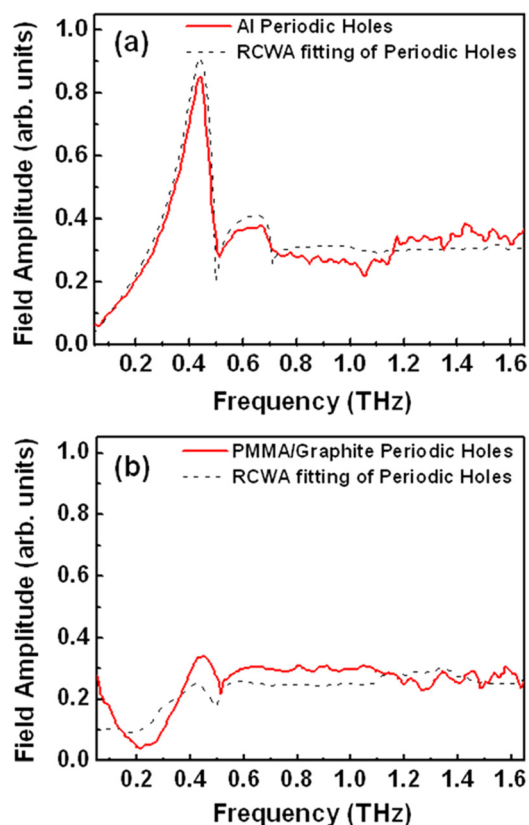


FIG. 5. (a) Normalized transmission spectra of Al film with $625 \mu\text{m}$ periodic holes (red). (b) Normalized transmission spectra of PMMA-graphite film with $613 \mu\text{m}$ periodic holes (red). Black dotted lines represent fitting results obtained using RCWA method.

IV. CONCLUSION

In order to understand, in detail, the role of dielectric properties of materials and the relative contributions of the surface property in transmission enhancement, we compared the THz transmissions through a freestanding perforated Al film and a PMMA-graphite composite film with various-sized holes. The absorptive material film with small-sized holes did not support any coupling between surface waves and transmitted field irrespective of that the hole arrays have periodicity. However, large-sized holes resulted in small field enhancement even in the absorptive material; this enhancement is similar to that in the case of metal hole arrays although it was weak. The different behaviors in the case of small and large holes can be explained with the fact that the transmissions can be affected by hole shape and periodicity simultaneously.

ACKNOWLEDGMENTS

This work was partially supported by the Korea Science and Engineering Foundation (KOSEF) (SRC, No. R11-2008-095-01000-0), KIST Institutional Programs (Project No. 2E25382), and the Center for Advanced Meta-Materials funded by the Ministry of Science, ICT and Future Planning as Global Frontier Project (Project No. 2014063727). We thank Professor Aurele J. L. Adam (TU Delft) and Professor Paul C. M. Planken for providing the THz near-field setup and their expertise. We also thank Professor Dai-Sik Kim

(Seoul National University) for his helpful comments and discussion.

- ¹T. W. Ebbesen, H. J. Lezec, H. F. Ghaemi, T. Thio, and P. A. Wolff, "Extraordinary optical transmission through sub-wavelength hole arrays," *Nature* **391**, 667–669 (1998).
- ²S. Collin, F. Pardo, R. Teissier, and J. L. Pelouard, "Strong discontinuities in the complex photonic band structure of transmission metallic gratings," *Phys. Rev. B* **63**, 033107 (2001).
- ³M. X. Qiu, S. C. Ruan, H. Su, C. D. Wang, M. Zhang, R. L. Wang, and H. W. Liang, "Enhanced transmission of THz radiation through sub-wavelength, asymmetry metallic hole arrays," *Appl. Phys. Lett.* **99**, 151501 (2011).
- ⁴J. W. Lee, M. A. Seo, J. Y. Sohn, Y. H. Ahn, D. S. Kim, S. C. Jeoung, C. Lienau, and Q. H. Park, "Invisible plasmonic meta-materials through impedance matching to vacuum," *Opt. Express* **13**, 10681–10687 (2005).
- ⁵D. R. Smith, J. B. Pendry, and M. C. K. Wiltshire, "Metamaterials and negative refractive index," *Science* **305**, 788–792 (2004).
- ⁶C. S. R. Kaipa, A. B. Yakovlev, G. W. Hanson, Y. R. Padooru, F. Medina, and F. Mesa, "Enhanced transmission with a graphene-dielectric micro-structure at low-terahertz frequencies," *Phys. Rev. B* **85**, 245407 (2012).
- ⁷J. Saxler, J. G. Rivas, C. Janke, H. P. M. Pellemans, P. H. Bolivar, and H. Kurz, "Time-domain measurements of surface plasmon polaritons in the terahertz frequency range," *Phys. Rev. B* **69**, 155427 (2004).
- ⁸J. G. Rivas, C. Schotsch, P. H. Bolivar, and H. Kurz, "Enhanced transmission of THz radiation through subwavelength holes," *Phys. Rev. B* **68**, 201306 (2003).
- ⁹Y. M. Shin, J. K. So, K. H. Jang, J. H. Won, A. Srivastava, and G. S. Park, "Superradiant terahertz Smith-Purcell radiation from surface plasmon excited by counterstreaming electron beams," *Appl. Phys. Lett.* **90**, 031502 (2007).
- ¹⁰J. B. Pendry, L. Martin-Moreno, and F. J. Garcia-Vidal, "Mimicking surface plasmons with structured surfaces," *Science* **305**, 847–848 (2004).
- ¹¹F. J. Garcia-Vidal, L. Martin-Moreno, and J. B. Pendry, "Surfaces with holes in them: New plasmonic metamaterials," *J. Opt. A* **7**, S97–S101 (2005).
- ¹²W. Cao, C. Song, T. E. Lanier, R. Singh, J. F. O'Hara, W. M. Dennis, Y. Zhao, and W. Zhang, "Tailoring terahertz plasmons with silver nanorod arrays," *Sci. Rep.* **3**, 1766 (2013).
- ¹³W. Zhu, A. Agrawal, and A. Nahata, "Planar plasmonic terahertz guided-wave devices," *Opt. Express* **16**, 6216–6226 (2008).
- ¹⁴X. Lu, R. Wan, G. Wang, T. Zhang, and W. Zhang, "Giant and tunable electric field enhancement in the terahertz regime," *Opt. Express* **22**, 27001–27006 (2014).
- ¹⁵D. Gacemi, J. Mangeney, R. Colombelli, and A. Degiron, "Subwavelength metallic waveguides as a tool for extreme confinement of THz surface waves," *Sci. Rep.* **3**, 1369 (2013).
- ¹⁶K. A. Abul, Y. Zhao, and W. Zhang, "Transmission properties of terahertz pulses through an ultrathin subwavelength silicon hole array," *Appl. Phys. Lett.* **86**, 141102 (2005).
- ¹⁷M. A. Seo, J. W. Lee, and D. S. Kim, "Dielectric constant engineering with polymethylmethacrylate-graphite metastate composites in the terahertz region," *J. Appl. Phys.* **99**, 066103 (2006).
- ¹⁸A. Das, C. M. Megaridis, L. Liu, T. Wang, and A. Biswas, "Design and synthesis of superhydrophobic carbon nanofiber composite coatings for terahertz frequency shielding and attenuation," *Appl. Phys. Lett.* **98**, 174101 (2011).
- ¹⁹J. W. Lee, M. A. Seo, D. S. Kim, S. C. Jeoung, C. Lienau, J. H. Kang, and Q. H. Park, "Fabry-Perot effects in THz time-domain spectroscopy of plasmonic band-gap structures," *Appl. Phys. Lett.* **88**, 071114 (2006).
- ²⁰J. W. Lee, M. A. Seo, D. J. Park, D. S. Kim, S. C. Jeoung, C. Lienau, Q. H. Park, and P. C. M. Planken, "Shape resonance omnidirectional terahertz filters with near-unity transmittance," *Opt. Express* **14**, 1253–1259 (2006).
- ²¹C. Y. Lee, H. G. Song, K. S. Jang, E. J. Oh, A. J. Epstein, and J. Joo, "Electromagnetic interference shielding efficiency of polyaniline mixtures and multilayer films," *Synth. Met.* **102**, 1346–1349 (1999).
- ²²H. C. F. Martens, J. A. Reedijk, H. B. Brom, D. M. D. Leeuw, and R. Menon, "Metallic state in disordered quasi-one-dimensional conductors," *Phys. Rev. B* **63**, 073203 (2001).
- ²³M. A. Seo, A. J. L. Adam, J. H. Kang, J. W. Lee, S. C. Jeoung, Q. H. Park, P. C. M. Planken, and D. S. Kim, "Fourier-transform terahertz near-field

- imaging of one-dimensional slit arrays: mapping of electric-field-, magnetic-field-, and Poynting vectors," *Opt. Express* **15**, 11781–11789 (2007).
- ²⁴P. C. M. Planken, H. K. Nienhuys, H. J. Bakker, and T. Wenckebach, "Measurement and calculation of the orientation dependence of terahertz pulse detection in ZnTe," *J. Opt. Soc. Am. B* **18**, 313–317 (2001).
- ²⁵H. Cao and A. Nahata, "Resonantly enhanced transmission of terahertz radiation through a periodic array of subwavelength apertures," *Opt. Express* **12**, 1004–1010 (2004).
- ²⁶H. Giovannini and C. Amra, "Dielectric thin films for maximized absorption with standard quality black surfaces," *Appl. Opt.* **37**, 103–105 (1998).
- ²⁷M. G. Moharam, D. A. Pommet, E. B. Grann, and T. K. Gaylord, "Stable implementation of the rigorous coupled-wave analysis for surface-relief gratings: Enhanced transmittance matrix approach," *J. Opt. Soc. Am. A* **12**, 1077–1086 (1995).
- ²⁸J. W. Lee, M. A. Seo, D. H. Kang, K. S. Khim, S. C. Jeoung, and D. S. Kim, "Terahertz electromagnetic wave transmission through random arrays of single rectangular holes and slits in thin metallic sheets," *Phys. Rev. Lett.* **99**, 137401 (2007).
- ²⁹K. J. K. Koerkamp, S. Enoch, F. B. Segerink, N. F. van Hulst, and L. Kuipers, "Strong influence of hole shape on extraordinary transmission through periodic arrays of subwavelength holes," *Phys. Rev. Lett.* **92**, 183901 (2004).